AIMS Mathematics, 9(3): 5971–5994.
DOI:10.3934/math.2024292
Received: 26 November 2023
Revised: 22 January 2024
Accepted: 24 January 2024
Published: 01 February 2024

http://www.aimspress.com/journal/Math

Research article

Preserving monotone or convex data using quintic trigonometric Bézier curves

Salwa Syazwani Mahzir[1], **Md Yushalify Misro**[1,2,*] **and Kenjiro T. Miura**[2]

[1] School of Mathematical Sciences, Universiti Sains Malaysia, 11800 Gelugor, Pulau Pinang, Malaysia

[2] Department of Mechanical Engineering, Shizuoka University, Hamamatsu 432-8561, Shizuoka, Japan

* **Correspondence:** Email: yushalify@usm.my.

Abstract: Bézier curves are essential for data interpolation. However, traditional Bézier curves often fail to detect special features that may exist in a data set, such as monotonicity or convexity, leading to invalid interpolations. This study aims to improve the deficiency of Bézier curves by imposing monotonicity or convexity-preserving conditions on the shape parameter and control points. For this purpose, the quintic trigonometric Bézier curves with two shape parameters are used. These techniques constrain only one of the shape parameters, leaving the other free to provide users with more freedom and flexibility in modifying the final curve. To guarantee smooth interpolation, the curvature profiles of the curves are analyzed, which aids in selecting the optimal shape parameter values. The effectiveness of the developed schemes was evaluated by implementing real-life data and data obtained from the existing schemes. Compared with the existing schemes, the developed schemes produce low-curvature interpolation curves with unnoticeable wiggles and turns. The proposed methods also work effectively for both nonuniformly spaced data and negative-valued convex data in real-life applications. When the shape parameter is correctly chosen, the developed interpolants exhibit continuous curvature plots, assuring C^2 continuity.

Keywords: monotonicity-preserving; convexity-preserving; quintic trigonometric Bézier; shape-preserving interpolation; shape parameter; curvature
Mathematics Subject Classification: 65D05, 65D07, 65D17, 68U07

1. Introduction

Shape-preserving interpolation is a fundamental concept in numerical analysis and data approximations. It is essential for maintaining the important characteristics of a dataset while

generating a continuous function that smoothly connects all data points. Monotone data, such as the uric acid level in gout patients [1] and the rate of radioactive decay [2], exhibits a consistent directional trend, either increasing or decreasing, whereas convex data shows a curve that slopes upward. The problem of convex data arises in the design of telecommunication systems, parameter estimation, and approximation theory [3]. Preserving monotonicity and convexity ensures that the interpolated function accurately represents the fundamental behavior of the original data. This field has been revolutionized over the years, improving the way data is interpolated.

The study of monotonicity preservation by [4] proposed a monotonicity-preserving technique using a C^1-weighted quadratic spline. As the developed technique is non-rational, it is easy to implement and requires less computational time. [5] presented a monotonicity-preserving technique that achieved GC^1 continuity by employing a rational quartic over linear spline function. [6, 7] implemented cubic over linear and quadratic rational functions, resulting in C^2 interpolant with the unknown derivative values determined by solving a system of tridiagonal equations. [8,9] constructed C^1 monotonicity-preserving schemes using (cubic/cubic) and (cubic/quadratic) rational cubic Ball interpolation functions. By having more free parameters, [9] provided greater flexibility for users to modify the resulting curves. On the other hand, [8, 10] provided curvature profile comparisons to quantitatively analyze the smoothness of the resulting curves. This approach eliminates the potential biases that may arise from subjective human judgment, providing a more reliable assessment of the curves' smoothness.

Further, subdivision schemes are also common in shape-preserving interpolation due to their ease of use and flexibility. [11] and [12] employed ternary and four-point ternary nonstationary interpolating subdivision schemes for monotonicity-preserving schemes. Furthermore, fractal splines are employed in monotonicity-preserving interpolation. [13, 14] created monotonicity-preserving interpolation algorithms based on a rational cubic fractal spline. These schemes involve the scaling and shape parameters. The latter scheme is more flexible because it sets limits only on the shape parameters, thereby leaving the scaling factor free for curve adjustment.

A C^1 convexity-preserving piecewise variable-degree rational interpolation spline with two local shape parameters was developed by [15]. Due to the positive second derivatives of the interpolant, the convex data can be directly preserved. Rational cubic and quartic interpolants were used by [16–18]. A C^1 continuous convexity preserving scheme was developed by [16], whereas [17, 18] developed C^2 continuous schemes. [17] used LU decomposition to solve for the derivative values, while [18] offered a simpler approach that yields a local scheme by directly computing the derivative values. [19] implemented a trigonometric function with a shape parameter. This approach is rigid because the shape parameter is constrained to preserve convexity. [20] suggested convexity-preserving methods for generalized cubic spline, including rational, exponential, variable power, hyperbolic, and spline with additional knots. The non-convex curve segments are adjusted with near-optimal tension parameters. The developed scheme is universal and can be applied to any type of generalized spline with tension parameters.

First introduced in 1958, Bézier curves have gotten considerable attention due to their simple development and ease of control due to their convex hull properties. In addition, no advanced knowledge of computer aided geometric design (CAGD) is needed to use the curves because they are made up of control points and Bernstein polynomials, which can be easily developed. In addition to the conventional Bézier curve, trigonometric Bézier curves with shape parameters have been proposed [21–23], resulting in greater adjustability and control of the curve shape. Because of the

nice properties they hold, Bézier curves have been applied to many real-life applications, including highway design [24], path planning [25], image compression [26], and surface construction [27]. However, when applied to data interpolations, Bézier curves neglect important features of the data, resulting in misleading interpolation. This study aims to incorporate the shape-preserving approach into the trigonometric Bézier curves by developing data-dependent constraints on the shape parameter and introducing a scaling factor on the control points to ensure the control points' monotonicity or convexity. Curvature analysis is also conducted to assess the smoothness of the resulting interpolation.

This paper is structured as follows: In Section 2, the C^2 quintic trigonometric Bézier interpolating curve is constructed, and the method for computing the derivative values is explained. Next, the derivation of the monotonicity or convexity-preserving conditions for the shape parameter is presented in Section 3. The formula for computing the curvature profile is described in Section 4. Section 5 presents graphical examples of shape-preserving interpolations by implementing new and previous data sets from the existing scheme. Finally, Section 6 provides the conclusion and a few possible directions for further research.

2. C^2 quintic trigonometric Bézier curve with two shape parameters

For the purpose of this study, the quintic trigonometric Bézier curve with two shape parameters proposed by [23] will be used. Let $\{(x_i, y_i) : i = 0, 1, 2, \ldots, n\}$ be a set of data defined over the interval $[x_0, x_n]$ with $x_{i+1} > x_i$. The quintic trigonometric Bézier curve in each subinterval $I_i = [x_i, x_{i+1}]$ is given by

$$s(x) \equiv s_i(x) = \sum_{j=0}^{5} \boldsymbol{B_j} f_j(x), \tag{2.1}$$

where $\boldsymbol{B_j}$ and $f_j(x)$ denote the control points and the basis functions of the quintic trigonometric Bézier curves that are given as follows:

$$\begin{aligned}
f_0(x) &= (1 - \sin\theta)^4 (1 - \alpha \sin\theta), \\
f_1(x) &= \sin\theta (1 - \sin\theta)^3 (4 + \alpha - \alpha \sin\theta), \\
f_2(x) &= (1 - \sin\theta)^2 (1 - \cos\theta)(8 \sin\theta + 3\cos\theta + 9), \\
f_3(x) &= (1 - \cos\theta)^2 (1 - \sin\theta)(8 \cos\theta + 3\sin\theta + 9), \\
f_4(x) &= \cos\theta (1 - \cos\theta)^3 (4 + \beta - \beta \cos\theta), \\
f_5(x) &= (1 - \cos\theta)^4 (1 - \beta \cos\theta),
\end{aligned} \tag{2.2}$$

where $\theta = \dfrac{\pi(x - x_i)}{2h_i}$ with $\theta \in [0, \dfrac{\pi}{2}]$. The shape parameters $\alpha, \beta \in [-4, 1]$ are responsible for controlling the shape of the curve. The quintic trigonometric Bézier basis functions, $f_j(x)$ for $j = 0, 1, 2, 3, 4, 5$ in Eq (2.2), have the following geometric properties:

(1) Non-negativity:

$$f_j(x) \geq 0 \text{ for all } x \in [x_i, x_{i+1}].$$

(2) Symmetry:

$$f_j(x) = f_{5-j}(x_{i+1} - x) \text{ if } \alpha = \beta.$$

(3) Partition of unity:

$$\sum_{j=0}^{5} f_j(x) = 1 \text{ for all } x \in [x_i, x_{i+1}].$$

In addition, the quintic trigonometric Bézier curve in Eq (2.1) also satisfies other properties such as the endpoint terminal, convex hull, symmetry, and geometric invariance, which were further discussed in [23]. The plot of the quintic trigonometric Bézier basis functions for various values of the shape parameters, α and β, is shown in Figure 1 below.

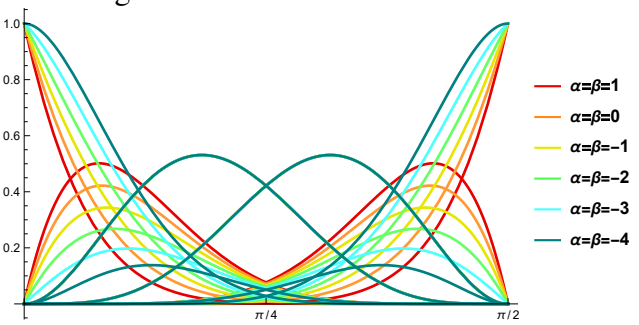

Figure 1. Quintic trigonometric Bézier basis functions.

Next, the C^2 interpolating conditions (2.3) will be applied to Eq (2.1) to determine the equations of the unknown control points $\boldsymbol{B_j}$. Let s' and s'' be the first-order and second-order derivatives of s, and the interpolating conditions are

$$\begin{aligned} s(x_i) &= y_i, \quad & s(x_{i+1}) &= y_{i+1}, \\ s'(x_i) &= d_i, \quad & s'(x_{i+1}) &= d_{i+1}, \\ s''(x_i) &= D_i, \quad & s''(x_{i+1}) &= D_{i+1}, \end{aligned} \tag{2.3}$$

where d_i and D_i are the first-order and second-order derivative values at knots.

Taking into account the local variable relative to I_i, from Eqs (2.1)–(2.3) it is straightforward to establish that

$$\begin{aligned} \boldsymbol{B_0} &= y_i, \\ \boldsymbol{B_1} &= y_i + \frac{2h_i d_i}{(4+\alpha_i)\pi}, \\ \boldsymbol{B_2} &= y_i + \frac{h_i\left((4+\alpha_i)D_i h_i + 4(3+\alpha_i)d_i\pi\right)}{3(4+\alpha_i)\pi^2}, \\ \boldsymbol{B_3} &= y_{i+1} - \frac{h_i\left((\beta_i-4)D_{i+1}h_i + 4(3+\beta_i)d_{i+1}\pi\right)}{3(4+\beta_i)\pi^2}, \\ \boldsymbol{B_4} &= y_{i+1} - \frac{2h_i d_{i+1}}{(4+\beta_i)\pi}, \\ \boldsymbol{B_5} &= y_{i+1}, \end{aligned} \tag{2.4}$$

with $h_i = x_{i+1} - x_i$.

As a result, the C^2 quintic trigonometric Bézier curve with two shape parameters in Eq (2.1) defined

over each subinterval I_i can be written as

$$\begin{aligned} s(x) = \sum_{j=0}^{5} \boldsymbol{B}_j f_j(x) = {} & y_i (1-\sin\theta)^4 (1-\alpha_i \sin\theta) + \left(y_i + \frac{2h_i d_i}{(4+\alpha_i)\pi}\right) \sin\theta (1-\sin\theta)^3 \\ & (4+\alpha_i-\alpha_i \sin\theta) + \left(y_i + \frac{h_i((4+\alpha_i)D_i h_i + 4(3+\alpha_i)d_i\pi)}{3(4+\alpha_i)\pi^2}\right)(1-\sin\theta)^2 (1-\cos\theta) \\ & (8\sin\theta + 3\cos\theta + 9) + \left(y_{i+1} + \frac{h_i((4+\beta_i)D_{i+1}h_i - 4(3+\beta_i)d_{i+1}\pi)}{3(4+\beta_i)\pi^2}\right)(1-\cos\theta)^2 \\ & (1-\sin\theta)(8\cos\theta + 3\sin\theta + 9) + \left(y_{i+1} - \frac{2h_i d_{i+1}}{(4+\beta_i)\pi}\right)\cos\theta (1-\cos\theta)^3 \\ & (4+\beta_i-\beta_i\cos\theta) + y_{i+1}(1-\cos\theta)^4 (1-\beta_i\cos\theta). \end{aligned} \tag{2.5}$$

2.1. Determination of derivative values

In this research, the values of d_i and D_i are both calculated from the given data using the arithmetic mean method (AMM).

From [28], the first-order derivative values at the first knot are as follows:

$$d_0 = \Delta_0 + (\Delta_0 - \Delta_1)\frac{h_0}{h_0 + h_1}, \tag{2.6}$$

$$d_i = \frac{\Delta_i + \Delta_{i+1}}{2} \text{ for } i = 1, 2, \ldots, n-1, \tag{2.7}$$

$$d_n = \Delta_{n-1} + (\Delta_{n-1} - \Delta_{n-2})\frac{h_{n-1}}{h_{n-1} + h_{n-2}}, \tag{2.8}$$

where $\Delta_i = \dfrac{y_{i+1} - y_i}{h_i}$.

Meanwhile, the second-order derivative values at the first knot are given by the following [28]:

$$D_0 = M_0 + (M_0 - M_1)\frac{h_0}{h_0 + h_1}, \tag{2.9}$$

$$D_i = \frac{M_i + M_{i+1}}{2} \text{ for } i = 1, 2, \ldots, n-1, \tag{2.10}$$

$$D_n = M_{n-1} + (M_{n-1} - M_{n-2})\frac{h_{n-1}}{h_{n-1} + h_{n-2}}, \tag{2.11}$$

with $M_i = \dfrac{d_{i+1} - d_i}{h_i}$.

3. Shape preserving interpolation using C^2 quintic trigonometric Bézier curves

The C^2 quintic trigonometric Bézier curve constructed in Section 2 does not guarantee data-shape preservation. Therefore, this section will develop shape-preserving constraints, specifically on the shape parameter α_i, which controls the left end of the interpolation curves. The shape parameter β_i, which controls the right-end part of the curves, will remain flexible to allow modification of the resulting curve according to the user's preference. Moreover, the control points will also be restricted and automatically calculated for shape preservation.

3.1. Monotonicity-preserving C^2 quintic trigonometric Bézier curves

Suppose (x_i, y_i) is a monotonically increasing data set such that

$$y_{i+1} \geq y_i \text{ with } x_{i+1} \geq x_i. \tag{3.1}$$

Thus, it is straightforward to establish that $\Delta_i \geq 0$ and $d_i \geq 0$.

Theorem 3.1. *The C^2 quintic trigonometric Bézier curves defined in Eq (2.5) will preserve the monotonicity of monotone data if the parameters α_i, β_i, $\bar{h}_i$, and $\bar{h}_i^*$ in each subinterval satisfy the following conditions:*
$\beta_i \in (-4, 1]$, which produces a monotone curve, and $\alpha_i \in [l_i, u_i]$ for

$$l_i = \min\left\{0, \frac{-2h_i d_i}{\pi y_i} - 4, \frac{4\pi h_i d_i}{3\pi^2 y_i + 4\pi d_i h_i + D_i h_i^2} - 4\right\}, \tag{3.2}$$

$$u_i = \max\left\{1, \frac{-2h_i d_i}{\pi y_i}, \frac{4\pi h_i d_i}{3\pi^2 y_i + 4\pi d_i h_i + D_i h_i^2}\right\}. \tag{3.3}$$

Let b_j for $j = 1, 2, 3, 4$ be the second terms in $\boldsymbol{B_j}$

$$\begin{cases} \bar{h}_i = \dfrac{h_i}{k_i}, & \text{if } b_1 > \dfrac{dy_i}{2} \text{ or } b_2 > \dfrac{dy_i}{2}, \\ \bar{h}_i^* = \dfrac{h_i}{k_i^*}, & \text{if } b_3 > \dfrac{dy_i}{2} \text{ or } b_4 > \dfrac{dy_i}{2}, \\ \bar{h}_i = \bar{h}_i^* = h_i, & \text{elsewhere}, \end{cases} \tag{3.4}$$

where k_i, k_i^* satisfy Eqs (3.9) and (3.10).

Proof. The C^2 quintic trigonometric Bézier curves (2.5) will preserve the monotonicity of data if

$$s^{(1)}(x) \geq 0.$$

Differentiating $s(x)$ with respect to x results in 16 terms that are associated with both shape parameters α_i and β_i. As this study aims to constrain only the shape parameter α_i, only eight terms that are associated with the shape parameter, α_i, are considered, as given by the following equation:

$$s_\alpha^{(1)}(x) = \sum_{j=0}^{7} A_j k_j(x) \geq 0, \tag{3.5}$$

where $k_j(x)$ for $j = 0, 1, 2, \ldots, 7$ are non-negative functions defined in Eq (3.6). The plot of the functions is demonstrated in Figure 2.

$$\begin{aligned} k_0(x) &= \cos\theta(1 - \sin\theta)^4, \\ k_1(x) &= \cos\theta \sin\theta(1 - \sin\theta)^3, \\ k_2(x) &= (1 - \cos\theta)\cos\theta(1 - \sin\theta)(9 + 3\cos\theta + 8\sin\theta), \\ k_3(x) &= (1 - \sin\theta)^2 \sin\theta(9 + 3\cos\theta + 8\sin\theta), \\ k_4(x) &= (1 - \cos\theta)(1 - \sin\theta)^2(8\cos\theta - 3\sin\theta), \\ k_5(x) &= \cos\theta(1 - \sin\theta)^3(1 - \alpha\sin\theta), \\ k_6(x) &= \cos\theta(1 - \sin\theta)^3(4 + \alpha - \alpha\sin\theta), \\ k_7(x) &= \cos\theta(1 - \sin\theta)^2 \sin\theta(4 + \alpha - \alpha\sin\theta). \end{aligned} \tag{3.6}$$

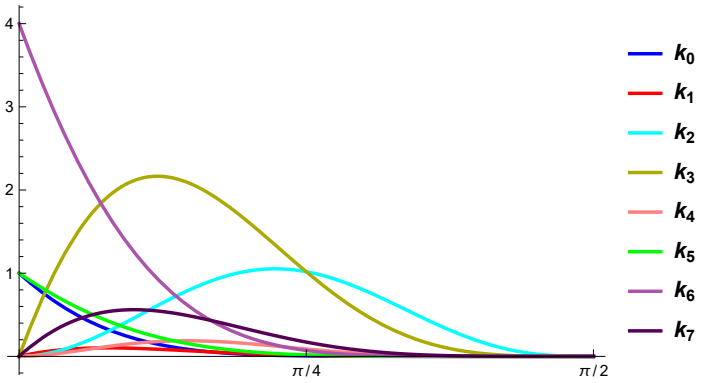

Figure 2. Plot of k_j functions.

Since $k_j(x)$ is already greater than zero, mathematical derivations are needed to ensure $A_j \geq 0$ for $j = 0, 1, 2, \ldots, 7$, hence, guaranteeing Eq (3.5). This will be done by letting $A_j \geq 0$ and solving for α_i.

(1) Let $A_0 = -\dfrac{\alpha_i \pi y_i}{2h_i} \geq 0$. Solving in terms of α_i results in $\alpha_i \leq 0$.

(2) $A_1 = -\dfrac{\alpha_i \pi \left(y_i + \dfrac{2d_i h_i}{(4+\alpha_i)\pi} \right)}{2h_i} \geq 0$. Simplified and rearranged, this yields $\alpha_i \leq \dfrac{-2h_i d}{\pi y_i} - 4$.

(3) For $A_2 = -\dfrac{\pi \left(y_i + \dfrac{h_i\,(4\pi(3+\alpha_i)d_i + (4+\alpha_i)h_i D_i)}{3\pi^2(4+\alpha_i)} \right)}{h_i} \geq 0$, solving for α_i gives $\alpha_i \leq \dfrac{4\pi h_i d_i}{h_i^2 D_i + 4\pi h_i d_i + 3\pi^2 y_i} - 4$.

(4) Then, $A_3 = A_4$. Letting these terms be greater than zero produces $A_3 = A_4 = \dfrac{\pi \left(y_i + \dfrac{h_i\,(4\pi(3+\alpha_i)d_i + (4+\alpha_i)h_i D_i)}{3\pi^2(4+\alpha_i)} \right)}{2h_i} \geq 0$. Rearrangement and simplifications result in $\alpha_i \geq \dfrac{4\pi h_i d_i}{h_i^2 D_i + 4\pi h_i d_i + 3\pi^2 y_i} - 4$, which acts as a lower bound for monotonicity preservation and can be simplified as $\alpha_i \geq \dfrac{4\pi h_i d_i}{h_i^2 D_i + 4\pi h_i d_i + 3\pi^2 y_i}$.

(5) $A_5 = \dfrac{2\pi y_i}{h_i}$ is already greater than zero.

(6) Let $A_6 \geq 0$, giving $A_6 = \dfrac{\pi \left(y_i + \dfrac{2h_i d_i}{(4+\alpha_i)\pi} \right)}{2h_i} \geq 0$. Next, solving in terms of α_i produces $\alpha_i \leq \dfrac{-2h_i d}{\pi y_i} - 4$.

(7) Lastly, for $A_7 = -\dfrac{3\pi \left(y_i + \dfrac{2h_i d_i}{(4+\alpha_i)\pi} \right)}{2h_i} \geq 0$, solving for α_i yields $\alpha_i \geq \dfrac{-2h_i d}{\pi y_i} - 4$, which acts as the

lower bound. This, can be simplified to $\alpha_i \geq \dfrac{-2h_i d}{\pi y_i}$.

To summarize, the constraints for α_i above can be written as:

$$\begin{aligned} &\alpha_i \leq \frac{-2h_i d}{\pi y_i} - 4, \quad \alpha_i \leq \frac{4\pi h_i d_i}{h_i^2 D_i + 4\pi h_i d_i + 3\pi^2 y_i} - 4, \quad \alpha_i \leq 0, \\ &\alpha_i \geq \frac{-2h_i d}{\pi y_i}, \quad \alpha_i \geq \frac{4\pi h_i d_i}{h_i^2 D_i + 4\pi h_i d_i + 3\pi^2 y_i}, \end{aligned} \tag{3.7}$$

which can be rearranged as below:

$$\begin{aligned} l_i &= \min\left\{\frac{-2h_i d_i}{\pi y_i} - 4, \frac{4\pi h_i d_i}{h_i^2 D_i + 4\pi h_i d_i + 3\pi^2 y_i} - 4, 0\right\}, \\ u_i &= \max\left\{\frac{-2h_i d_i}{\pi y_i}, \frac{4\pi h_i d_i}{h_i^2 D_i + 4\pi h_i d_i + 3\pi^2 y_i}\right\}, \\ u_i &\leq \alpha_i \leq l_i. \end{aligned} \tag{3.8}$$

Moreover, to ensure a monotonically increasing interpolation, the control points $\boldsymbol{B_j}$ for j=0, 1, 2, 3, 4, 5 also need to be monotonically increasing. For this purpose, new conditions for the control points will be developed. Let the second term in the control points $\boldsymbol{B_j}$ for $j = 1, 2, 3, 4$ be b_j and $dy_i = y_{i+1} - y_i$ be the vertical difference between two neighboring data points.

If b_1 or $b_2 > \dfrac{dy_i}{2}$, the control points $\boldsymbol{B_1}$ and $\boldsymbol{B_2}$ from Eq (2.4) will be greater than $\boldsymbol{B_5}$. Since $\boldsymbol{B_5} = y_{i+1}$, this will cause the interpolating curve to rise and drop, resulting in oscillation. Thus, to avoid this, a scaling factor will be introduced by replacing h_i in b_1 and b_2 with $\bar{h}_i = \dfrac{h_i}{k_i}$, where

$$k_i > \max\left\{\frac{4\pi h_i d_i}{(4+\alpha_i)\pi dy_i}, \frac{4(3+\alpha_i)h_i d_i + \sqrt{2h_i^2(8(3+\alpha_i)^2 d_i^2 + 3(4+\alpha_i)^2 D_i dy_i)}}{3(4+\alpha_i)\pi dy_i}\right\}. \tag{3.9}$$

These constraints are developed by letting b_1 and $b_2 < \dfrac{dy_i}{2}$. Similarly, if b_3 or $b_4 > \dfrac{dy_i}{2}$, new scaling factor $\bar{h}_i^* = \dfrac{h_i}{k_i^*}$ will be developed by assuming b_3 and $b_4 < \dfrac{dy_i}{2}$ such that

$$k_i^* > \max\left\{\frac{4\pi h_i d_{i+1}}{(4+\beta_i)\pi dy_i}, \frac{4(3+\beta_i)h_i d_{i+1} + \sqrt{2h_i^2(8(3+\beta_i)^2 d_{i+1}^2 + 3(4+\beta_i)^2 D_{i+1} dy_i)}}{3(4+\beta_i)\pi dy_i}\right\}. \tag{3.10}$$

□

3.2. Convexity-preserving C^2 quintic trigonometric Bézier curves

A given data set $\{(x_i, y_i) : i = 0, 1, 2, \ldots, n\}$ is said to be convex if

$$\Delta_{i+1} \geq \Delta_i \quad \text{and} \quad d_{i+1} \geq d_i \quad \text{with} \quad d_{i+1} \geq \Delta_i \geq d_i, \tag{3.11}$$

for $i = 0, 1, 2, \ldots, n$ [19]. Graphically, a convex curve can be verified by connecting any two points on the curve. If none of the lines lie below the curve, then it is convex. Theorem 3.2 presents the convexity-preserving interpolation method.

Theorem 3.2. *The C^2 quintic trigonometric Bézier curves defined in Eq (2.5) will preserve the convexity of convex data if the parameters α_i, β_i, $\bar{h}_i$, and $\bar{h}_i^*$ in each subinterval satisfy the following conditions:*
$\beta_i \in (-4, 1]$, which produces a smooth and convex curve, and $\alpha_i \in [l_i, u_i]$, where

$$l_i = \frac{-2h_i d_i}{\pi y_i} - 4, \tag{3.12}$$

$$u_i = \max\left\{0, \frac{4\pi h_i d_i}{h_i^2 D_i + 4\pi h_i d_i + 3\pi^2 y_i}\right\}. \tag{3.13}$$

Let b_j for $j = 1, 2, 3, 4$ be the second terms of Eq (2.4). If $d_i > 0$,

$$\begin{cases} \bar{h}_i = \dfrac{h_i}{k_i}, & \text{if } b_1 > \dfrac{dy_i}{2} \text{ or } b_2 > \dfrac{dy_i}{2}, \\ \bar{h}_i^* = \dfrac{h_i}{k_i^*}, & \text{if } b_3 > \dfrac{dy_i}{2} \text{ or } b_4 > \dfrac{dy_i}{2}, \\ \bar{h}_i = \bar{h}_i^* = h_i, & \text{elsewhere}, \end{cases} \tag{3.14}$$

where k_i, k_i^* are defined as (3.9) and (3.10). If $d_i < 0$,

$$\begin{cases} \bar{h}_i = \dfrac{h_i}{k_i}, & \text{if } b_1 < \dfrac{dy_i}{2} \text{ or } b_2 < \dfrac{dy_i}{2}, \\ \bar{h}_i^* = \dfrac{h_i}{k_i^*}, & \text{if } b_3 < \dfrac{dy_i}{2} \text{ or } b_4 < \dfrac{dy_i}{2}, \\ \bar{h}_i = \bar{h}_i^* = h_i, & \text{elsewhere}, \end{cases} \tag{3.15}$$

for k_i, k_i^* given in Eqs (3.21) and (3.22).

Proof. The C^2 quintic trigonometric Bézier curves will preserve data convexity if

$$s^{(2)}(x) \geq 0. \tag{3.16}$$

Second-order differentiation of $s(x)$ with respect to x produces 18 terms associated with shape parameters α_i and β_i. Similarly, only the terms associated with α_i will be considered, as given:

$$s_\alpha^{(2)}(x) = \sum_{j=0}^{9} C_j g_j(x), \tag{3.17}$$

where $g_j(x)$ for $j = 0, 1, 2, \ldots, 8$ are defined as follows:

$$\begin{aligned}
g_0(x) &= \cos^2\theta(1-\sin\theta)^3,\\
g_1(x) &= (1-\sin\theta)^4\sin\theta,\\
g_2(x) &= \cos\theta(1-\sin\theta)^2(9+3\cos\theta+8\sin\theta),\\
g_3(x) &= (4+\alpha_i-\alpha_i\sin\theta)(6\pi^2\cos^2\theta(1-\sin\theta)+3\pi^2(1-\sin\theta)^2\sin\theta),\\
g_4(x) &= (1-\alpha_i\sin\theta)\left(3\pi^2\cos^2\theta(1-\sin\theta)^2+\pi^2(1-\sin\theta)^3\sin\theta\right),\\
g_5(x) &= \frac{1}{2}\pi^2(-1+\sin\theta)\sin\theta\,(3+9\cos 2\theta+6\sin\theta+4\cos\theta(5+12\sin\theta)),\\
g_6(x) &= \cos\theta(1-\sin\theta)^2\,(-\alpha_i\pi\cos\theta\sin\theta+\pi\cos\theta(4+\alpha_i-\alpha_i\sin\theta)),\\
g_7(x) &= (1-\sin\theta)^3\left(2\alpha_i\pi^2\cos^2\theta-\alpha_i\pi^2\sin^2\theta+\pi^2\sin\theta(4+\alpha_i-\alpha_i\sin\theta)\right),\\
g_8(x) &= -\pi^2\sin^2\frac{\theta}{2}(-1+\sin\theta)(44+6\cos\theta-72\cos 2\theta+88\sin\theta+27\sin 2\theta).
\end{aligned} \tag{3.18}$$

Similarly, the functions of $g_j(x)$ in Eq (3.18) are greater than or equal to zero. Thus, to guarantee Inequality (3.16) holds, derivations will be made so that C_j for $j = 0, 1, 2, \ldots, 8$ are greater than or equal to zero.

(1) Let $C_0 = \dfrac{2\alpha_i\pi^2 y_i}{h_i^2} \geq 0$. Solving in terms of α_i results in $\alpha_i \geq 0$.

(2) Similarly, $C_1 = \dfrac{\alpha_i\pi^2 y_i}{4h_i^2} \geq 0$ gives $\alpha_i \geq 0$.

(3) For $C_2 = \dfrac{\pi^2\left(y_i + \dfrac{h_i\,(4\pi(3+\alpha_i)d_i + (4+\alpha_i)h_iD_i)}{3\pi^2(4+\alpha_i)}\right)}{4h_i^2} \geq 0$, solving for α_i produces $\alpha_i \geq \dfrac{4\pi h_i d_i}{h_i^2 D_i + 4\pi h_i d_i + 3\pi^2 y_i}$.

(4) Next, assume $C_3 = \dfrac{y_i + \dfrac{2h_i d_i}{\pi(4+\alpha_i}}{4h_i^2} \geq 0$. Simplified and rearranged, this yields $\alpha_i \leq -\dfrac{2d_i h_i}{\pi y_i} - 4$.

(5) Because the data used is convex, $C_4 = y_i$ is convex.

(6) Let $C_5 = \dfrac{\pi\left(y_i + \dfrac{h_i\,(4\pi(3+\alpha_i)d_i + (4+\alpha_i)h_iD_i)}{3\pi^2(4+\alpha_i)}\right)}{2h_i^2} \geq 0$ and solve in terms of α_i, which gives $\alpha_i \geq \dfrac{4\pi h_i d_i}{h_i^2 D_i + 4\pi h_i d_i + 3\pi^2 y_i}$.

(7) Suppose $C_6 = \dfrac{3\pi\left(y_i + \dfrac{2h_i d_i}{\pi(4+\alpha_i)}\right)}{4h_i^2} \geq 0$, and after some rearrangements, this gives $\alpha_i \leq \dfrac{-2h_i d_i}{\pi y_i} - 4$.

(8) Rearrange $C_7 = -\dfrac{y_i + \dfrac{2h_i d_i}{\pi(4+\alpha_i)}}{4h_i^2} \geq 0$ in terms of α_i, which gives $\alpha_i \leq \dfrac{-2h_i d_i}{\pi y_i} - 4$.

(9) Finally, let $C_8 = \dfrac{y_i + \dfrac{h_i\,(4\pi(3+\alpha_i)d_i + (4+\alpha_i)h_i D_i)}{3\pi^2(4+\alpha_i)}}{4h_i^2} \geq 0$, and rearranging in terms of α_i results in $\alpha_i \geq \dfrac{4\pi h_i d_i}{h_i^2 D_i + 4\pi h_i d_i + 3\pi^2 y_i}$.

In summary, items (1)–(9) above can be written as:

$$\begin{aligned} &\alpha_i \leq \frac{-2h_i d}{\pi y_i} - 4, \\ &\alpha_i \geq 0, \quad \alpha_i \geq \frac{4\pi h_i d_i}{h_i^2 D_i + 4\pi h_i d_i + 3\pi^2 y_i}, \end{aligned} \tag{3.19}$$

which can be rearranged to produce the following conditions:

$$\begin{aligned} l_i &= \frac{-2h_i d_i}{\pi y_i} - 4, \\ u_i &= \max\left\{0, \frac{4\pi h_i d_i}{h_i^2 D_i + 4\pi h_i d_i + 3\pi^2 y_i}\right\}, \\ u_i &\leq \alpha_i \leq l_i. \end{aligned} \tag{3.20}$$

Next, the control points $\boldsymbol{B}_j$ for $j = 0, 1, 2, 3, 4, 5$ in Eq (2.4) for each subinterval must be set convex. Convex data are allowed to be monotonically increasing or decreasing in an interval. Thus, there are two cases to consider.

For the first case, which involves a monotonically increasing interval, the same conditions as in Eqs (3.9) and (3.10) will be applied. However, for monotone-decreasing interval, slight modifications will be made to the conditions. Suppose the second term in control points $\boldsymbol{B}_j$ for $j = 1, 2, 3, 4$ is b_j, and $dy_i = y_{i+1} - y_i$ is the vertical difference between two neighboring data points. In the monotone decreasing interval, $y_{i+1} \leq y_i$. Thus, $dy_i \leq 0$ and $d_i \leq 0$. Consequently, $b_j \leq 0$. If b_1 or $b_2 < \dfrac{dy_i}{2}$, or in other words, b_1 and b_2 are more negative than the half vertical difference, then y_i in (2.4) will be added with a number less than the negative vertical difference. Hence, b_1 and b_2 will be smaller than b_5, and the curve will drop and rise, which will produce a non-monotone interval. To prevent this, h_i in b_1 and b_2 will be replaced by $\bar{h_i} = \dfrac{h_i}{k_i}$, where k_i is the scaling factor introduced to ensure b_1 and $b_2 > \dfrac{dy_i}{2}$. Next, k_i is defined as follows:

$$k_i > \max\left\{\frac{4\pi h_i d_i}{(4+\alpha_i)\pi dy_i}, \frac{4(3+\alpha_i)h_i d_i - \sqrt{2h_i^2(8(3+\alpha_i)^2 d_i^2 + 3(4+\alpha_i)^2 D_i dy_i)}}{3(4+\alpha_i)\pi dy_i}\right\}. \tag{3.21}$$

Similarly, if b_3 or $b_4 < \dfrac{dy_i}{2}$, scaling factors $\bar{h_i^*} = \dfrac{h_i}{k_i^*}$ will be developed by assuming b_3 and $b_4 > \dfrac{dy_i}{2}$

such that

$$k_i^* > \max\left\{\frac{4\pi h_i d_{i+1}}{(4+\beta_i)\pi dy_i}, \frac{4(3+\beta_i)h_i d_{i+1} - \sqrt{2h_i^2(8(3+\beta_i)^2 d_{i+1}^2 + 3(4+\beta_i)^2 D_{i+1} dy_i)}}{3(4+\beta_i)\pi dy_i}\right\}. \tag{3.22}$$

□

Figure 3 depicts the flowchart of the proposed method to improve understanding. Algorithm 1 summarizes the method for generating C^2 monotonicity or convexity-preserving curves.

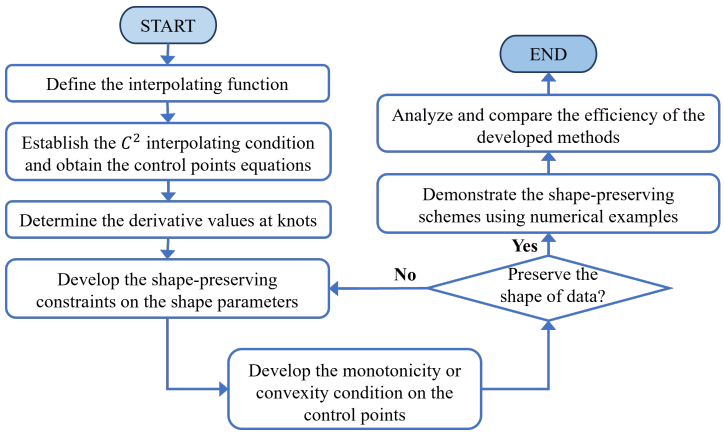

Figure 3. Flowchart of the shape-preserving interpolation schemes.

Algorithm 1 Monotonicity or convexity-preserving interpolation.

(1) Input data points $\{(x_i, y_i)\}_{i=0}^n$.
(2) Compute the values of $h_i = x_{i+1} - x_i$ and $\Delta_i = \dfrac{y_{i+1} - y_i}{h_i}$.
(3) Calculate first and second-order derivatives as discussed in Section 2.1.
(4) For each subinterval I_i, choose any value of $\beta_i \in (-4, 1]$.
(5) Calculate the values of parameters α_i and h_i based on Theorems 3.1 and 3.2.
(6) Construct the C^2 quintic trigonometric Bézier interpolating curve defined in (2.5) using the accumulated values obtained in Steps 1 to 5.

4. Curvature analysis

To ensure visually pleasing curves, this study implemented two ways of choosing the optimal β_i values: visual comparison and curvature analysis. For curvature analysis, the following formulation will be used to determine the smoothness. Let $s(x) = (s_x(x), s_y(x))$ be a $2D$ parametric curve of $s(x)$. The curvature of the curve, κ, is defined as follows:

$$\kappa(x) = \frac{|s'(x) \times s''(x)|}{|s'(x)|^3}, \tag{4.1}$$

which can also be expressed as

$$\kappa(x) = \frac{s_x'(x)s_y''(x) - s_x''(x)s_y'(x)}{\left[s_x'(x)^2 + s_y'(x)^2\right]^{3/2}}, \tag{4.2}$$

where $s'_x(x)$ and $s''_x(x)$ are the first and second-order partial derivatives of x. Meanwhile, $s'_y(x)$ and $s''_y(x)$ are the partial derivatives of y with respect to x.

5. Results and discussion

In this section, numerical experiments were conducted using MATLAB Software to assess the efficiency of the developed methods. Newly proposed data sets as well as data sets taken from the existing schemes were implemented for comparisons and validation.

Example 5.1. *Table 1 depicts a random monotone data set taken from [5].*

Table 1. Monotone data set from [5].

i	1	2	3	4	5
x	0	6	10	29.5	30
y	0.01	15	15	25	30

Example 5.2. *Table 2 provides an experimental data set of an electronic circuit's waveform distortion taken from [7]. The data demonstrated monotone increasing behavior with the x-values representing the voltage* (V)*, while the y-values are the current* (A)*.*

Table 2. Monotone data from [7].

i	1	2	3	4	5	6	7	8	9	10	11
x_i	0	2	3	5	6	8	9	11	12	14	15
y_i	10	10	10	10	10	10	10.5	15	50	60	85

Figures 4 and 5 show the interpolation of monotone data from Tables 1 and 2, respectively. Figures 4a and 5a show the interpolation curves using the traditional C^2 quintic trigonometric Bézier curves without satisfying the monotonicity-preserving constraints, where the shape parameters, α_i and β_i, in each subinterval, are set to 0.5. The interpolation curves fail to retain the monotonicity of the data, which can be observed in the third subinterval of Figure 4a as well as the seventh and ninth subintervals of Figure 5a. Figures 4b and 5b demonstrate the monotonicity preserving interpolation curves with the shape parameter α_i satisfying Theorem 3.1 for several β_i values within the interval $(-4, 1]$. The goal is to observe the best β_i values that give the smoothest interpolating curves.

From Figure 4b, it can be observed that all β_i values in the first subinterval produced similar interpolation curves. This is because the shape parameter β_i is associated with the right end of the curve. As the second subinterval is constant, the values of the first- and second-order derivatives are both zero. Consequently, changes in the shape parameter did not affect the last three control points of the subinterval. $\beta_i = -3.5$ and $\beta_i = -2.5$ in the third subinterval produce oscillating interpolations. Hence, this value must be avoided in the subinterval. By further examining the interpolation curves with varying values of β_i, the values of $\beta_i \in [-1.5, 0.5]$ are preferable because they produce a more visually pleasing interpolation. This can be proven using a curvature comparison, as shown in Figure 4c.

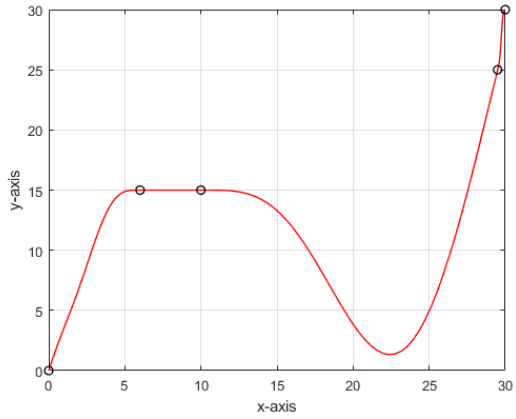

(a) Conventional C^2 quintic trigonometric Bézier interpolating curve.

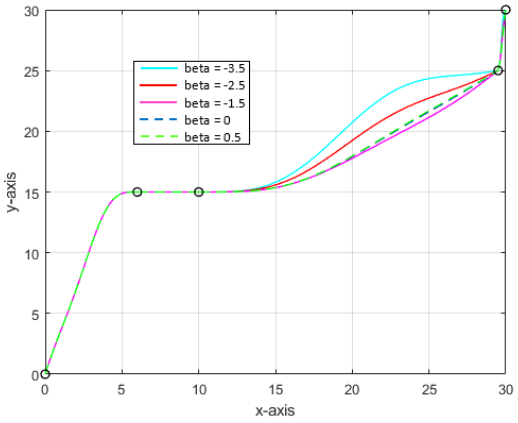

(b) Monotonicity-preserving interpolation with various β_i.

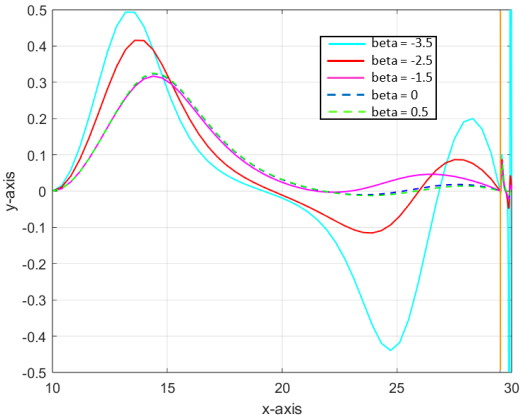

(c) Curvature plot for each curve in Figure 4b.

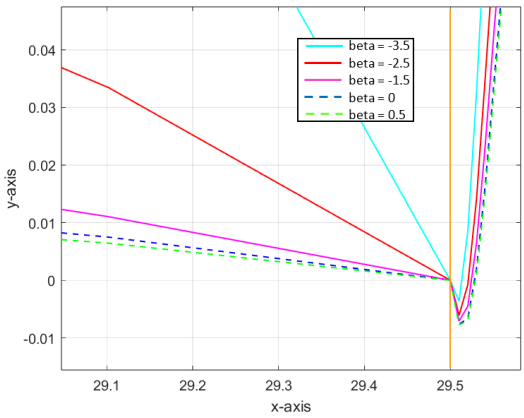

(d) Close-up of Figure 4c.

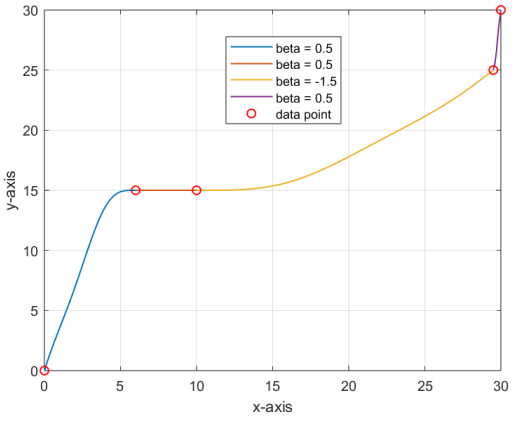

(e) Monotonicity-preserving interpolation with adjusted β_i.

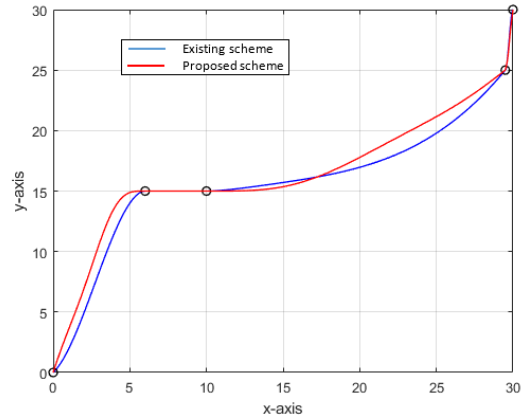

(f) Comparison with the scheme by [5].

Figure 4. Interpolations for Example 5.1.

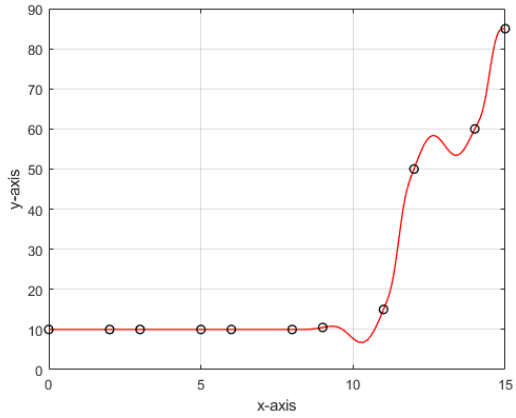

(a) Conventional C^2 quintic trigonometric Bézier interpolating curve.

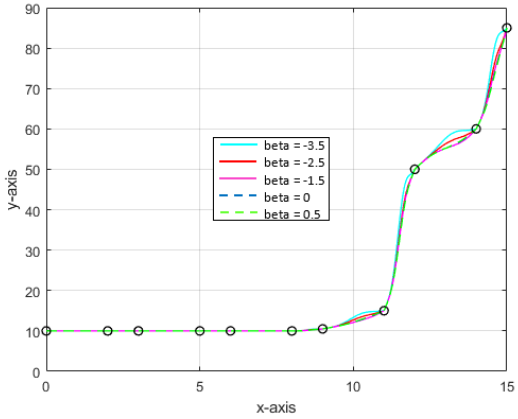

(b) Monotonicity-preserving interpolation with various β_i.

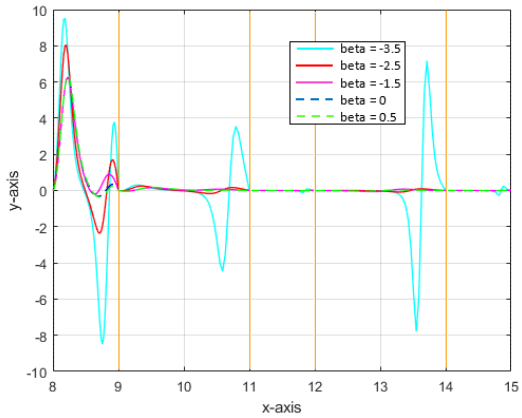

(c) Curvature plot for each curve in Figure 5b.

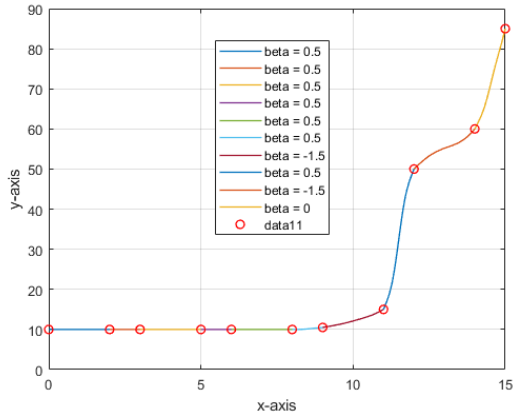

(d) Monotonicity-preserving interpolation with adjusted β_i.

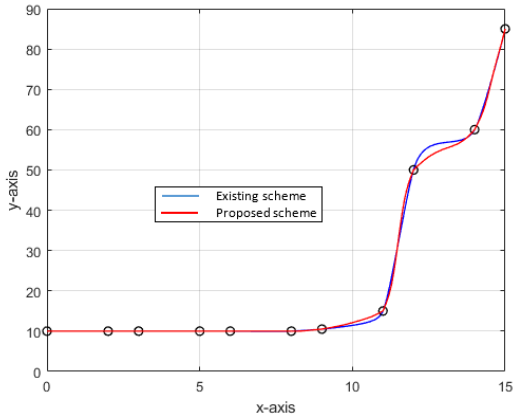

(e) Comparison with the scheme by [7].

Figure 5. Interpolations for Example 5.2.

The curvature plots for $\beta_i \in [-1.5, 0.5]$ have the lowest amplitude, indicating the smoothest curve. The interpolating curve with the optimal β_i values is shown in Figure 4e. Although $\beta_i = 0, 0.5$ have the lowest curvature for $x \in [22, 30]$, they result in a sharper curve than $\beta_i = -1.5$ because the low-curvature curve produces a straight curve towards the next data point. Thus, $\beta_i = -1.5$ in the third subinterval is the optimal value. As for the last subinterval, a sharp turn is observed at the joint due to the sudden increase in the data point over a small range of data. Despite this, the continuity of the curvature plot is still maintained, as shown in Figure 4d, confirming C^2 continuity.

For Example 5.2, flat data points are observed for subintervals $i = 1, 2, 3, \ldots, 6$ of Figure 5b. Hence, constant interpolation curves are obtained. The effect of applying different β_i values can be seen starting from the seventh subinterval onwards. Figure 5c illustrates the curvature plots of these subintervals with the vertical orange lines in the figure representing the partitions of the subintervals. $\beta_i \in [-1.5, 0.5]$ exhibits low curvature for the subintervals; hence, these values can be chosen. Figure 5d reflects the resulting monotonicity-preserving curves.

The developed method produced comparable interpolation with the existing scheme, as shown in Figure 4f. Further, compared to [7] in Figure 5e, the proposed method produced a smoother curve that increases gradually on the tenth subinterval.

Example 5.3. *Table 3 shows the cumulative rainfall data obtained from the Malaysian Meteorological Department, Ministry of Natural Resources, Environment and Climate Change. The data were taken at Bayan Lepas Station for 12 consecutive days from May 26 to June 6, 2022. The days are represented as x-values, whereas the y-values indicate the cumulative amount of rainfall measured in mm*^{3}*. Due to the non-negativity properties of the rainfall data, this data set is increasing monotonically.*

Table 3. Cumulative rainfall data.

i	1	2	3	4	5	6	7	8	9	10	11	12
x_i	1	2	3	4	5	6	7	8	9	10	11	12
y_i	1.8	3.2	3.2	3.2	11.6	16.6	48.2	67	68.4	90.8	92.8	92.9

Figure 6a interpolates the data set in Table 3 using the C^2 quintic trigonometric Bézier curves with $\alpha_i = \beta_i = 0.5$. Despite the monotonicity of the data, the interpolation curves in the fifth, eighth, and tenth subintervals exhibit fluctuations. These fluctuations are due to the large difference and sudden change in the y-values of the $i - 1$ and i subintervals.

Figure 6b illustrates the monotonicity-preserving interpolation with various values of the shape parameter β_i, while Figure 6c shows their curvature plots. Figure 6d shows the monotonicity-preserving interpolation with the best values of β_i that produce the most visually appealing curve with low curvature.

This data set has uniformly spaced x-values and inconsistent steepness of the y-values, making it different from the previous examples. Therefore, the proposed monotonicity-preserving method is efficient for both uniformly and nonuniformly spaced data points. Furthermore, the monotonicity of the data set is still preserved despite the large differences in the steepness of the data points.

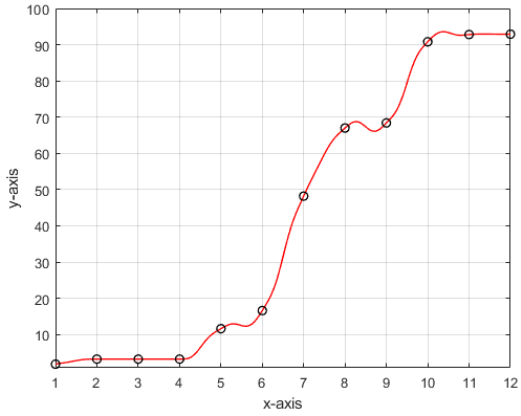

(a) Conventional C^2 quintic trigonometric Bézier interpolating curve.

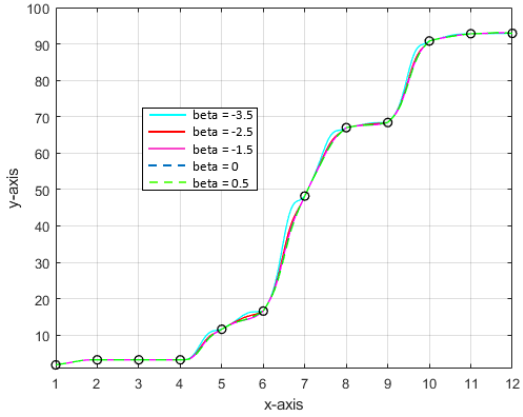

(b) Monotonicity-preserving interpolation with various β_i.

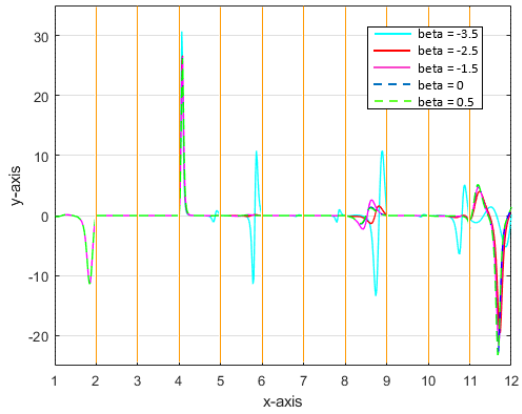

(c) Curvature plot for each curve in Figure 6b.

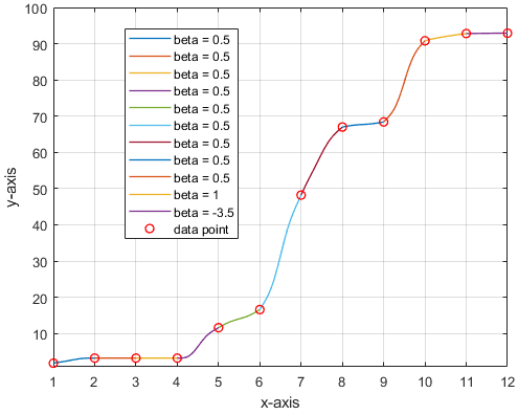

(d) Monotonicity-preserving interpolation with adjusted β_i.

Figure 6. Interpolations for Example 5.3.

Example 5.4. *Table 4 shows a convex data set taken from [19].*

Table 4. Convex data from [19].

i	1	2	3	4
x_i	3	4	5	7
y_i	7	0.4	0.4	2.5

Example 5.5. *Table 5 shows a data set generated by a convex function $f(x) = 10/x^2$ taken from [16].*

Table 5. Convex data from [16].

i	1	2	3	4	5
x_i	1	2	4	5	10
y_i	10	2.5	0.625	0.4	0.1

Figures 7 and 8 present the interpolation curves for the convex data in Tables 4 and 5, respectively.

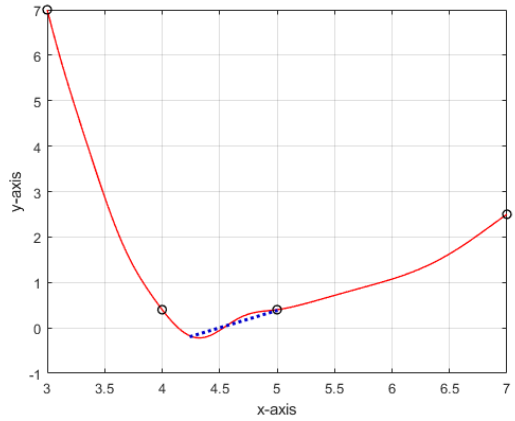

(a) Conventional C^2 quintic trigonometric Bézier interpolating curve.

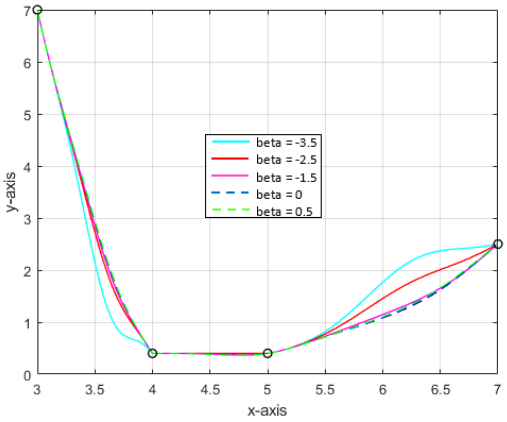

(b) Convexity-preserving interpolation with various β_i values.

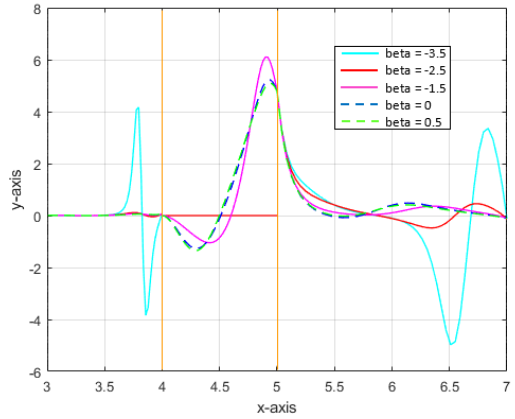

(c) Curvature plot for each curve in Figure 7b.

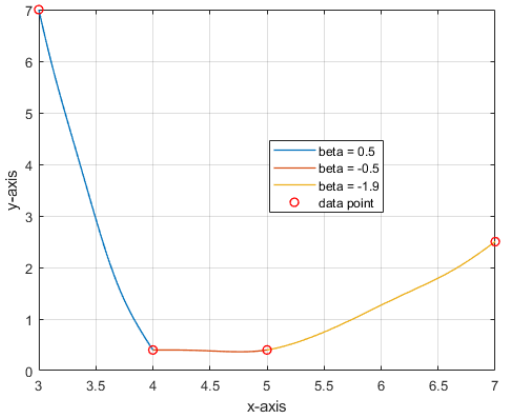

(d) Convexity-preserving interpolation with adjusted β_i.

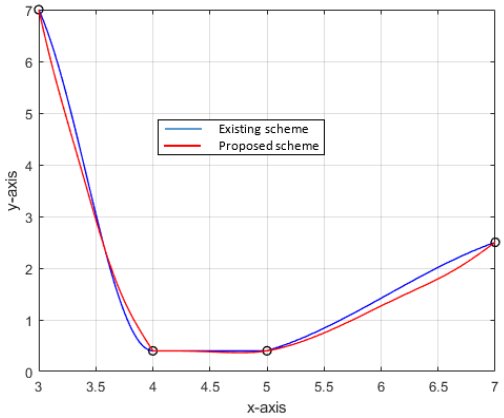

(e) Comparison with the scheme by [19].

Figure 7. Interpolations for Example 5.4.

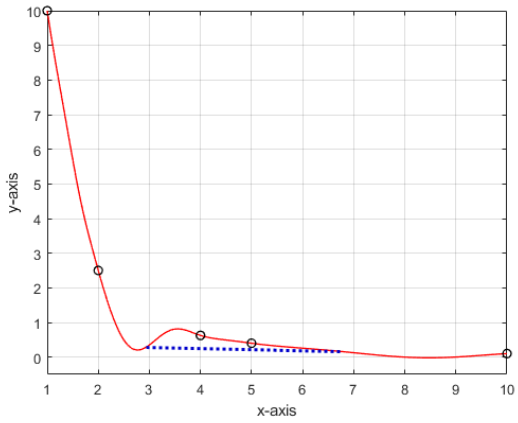

(a) Conventional C^2 quintic trigonometric Bézier interpolating curve

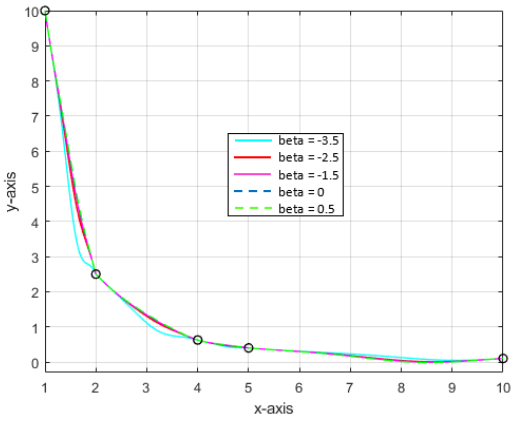

(b) Convexity-preserving interpolation with various β_i values.

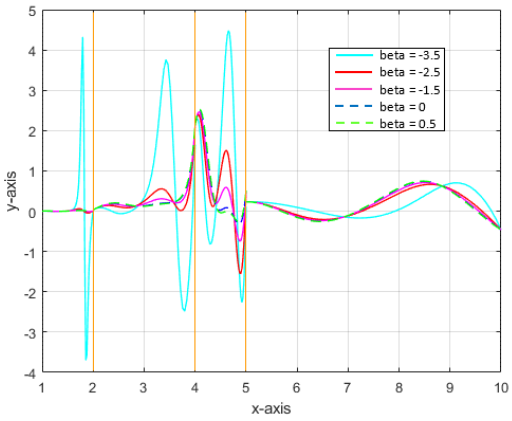

(c) Curvature plot for each curve in Figure 8b.

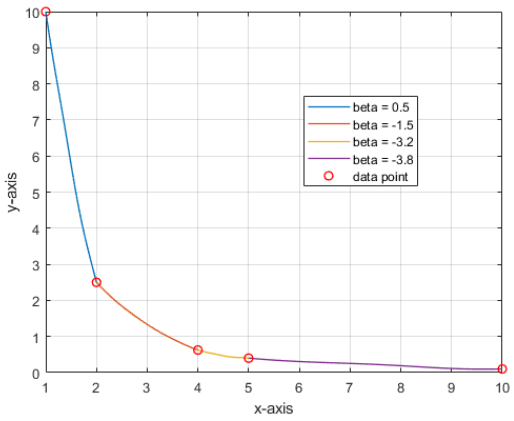

(d) Convexity-preserving interpolation with adjusted β_i.

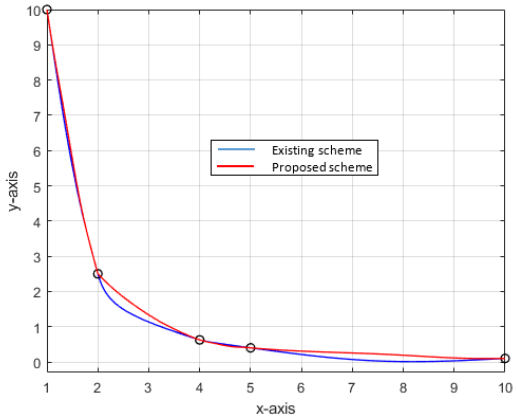

(e) Comparison with the scheme by [16].

Figure 8. Interpolations for Example 5.5.

Figures 7a and 8a demonstrate the failure of the C^2 quintic trigonometric Bézier curve to retain data convexity. As shown in the figures, the dotted blue lines connecting the two arbitrarily chosen points on the curves are below the curves. This contradicts the definition of convex curves.

Figures 7b and 8b show the convexity-preserving interpolations with several β_i values. β_i=−3.5, −2.5 in the third subinterval of Figure 7b result in non-convex interpolation. Moreover, from the curvature plot in Figure 7c, the values of β_i in the second subinterval produced disconnected curvature profiles, indicating failure in maintaining C^2 continuity due to the constant data points in the subinterval. Hence, these values of β_i must be avoided in both subintervals. $\beta_i \in [-1.5, 0.5]$ yielded the lowest curvature. Similarly, Figure 8c shows the curvature plot of the curves in Figure 8b. In Figures 7d and 8d, the curves were altered with the best β_i to obtain the smoothest C^2 interpolating curves.

Compared with existing schemes, the proposed method produces interpolation curves that are looser and smoother with no wiggle, as observed in the first and last subintervals of Figure 7e. This is because the proposed method uses degree-five interpolation curves with four intermediate control points; hence, it is more flexible and has greater control over the curve. Meanwhile, in Figure 8e, the curve of the proposed method is observed to be tighter, but in the second and fourth subintervals, the developed method displays a steady convex decreasing trend, giving a smooth-looking curve with unnoticeable turning.

Example 5.6. *The data of Toyota Prius rooftop measurements taken from [29] are shown in Table 6. The data were measured using a 3D laser scanner, and the data set exhibited a convex shape. In this study, only a subset of the collected data points was used to demonstrate the efficiency of the proposed method.*

Table 6. Car roof data.

i	1	2	3	4	5	6	7	8
x_i	1848.88	1948.09	1975.61	2516.23	2610.93	3068.07	3100.04	3279.18
y_i	-554.37	-575.38	-580.38	-632.013	-632.12	-593.84	-588.17	-548.09

Figure 9a shows the interpolation using the ordinary C^2 quintic trigonometric Bézier curves with shape parameters $\alpha_i = \beta_i = 0.5$. Non-convex interpolation can be seen in the third and fifth subintervals due to the large increment and decrement in the size of the data interval.

Figure 9b illustrates the convexity-preserving interpolation with varying β_i values to observe the optimal β_i. The resulting curves are analyzed quantitatively using the curvature plot shown in Figure 9c. The optimal β_i values are then chosen based on the observation and curvature plot to generate smooth convexity-preserving curves, as shown in Figure 9d. This example demonstrates that the proposed method is effective not only for positively valued convex data but also for negatively valued convex data.

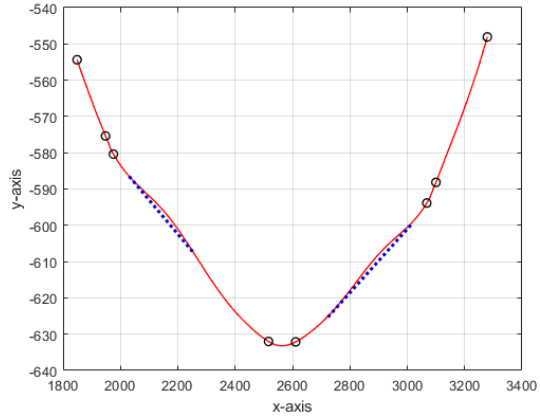

(a) Conventional C^2 quintic trigonometric Bézier interpolating curve.

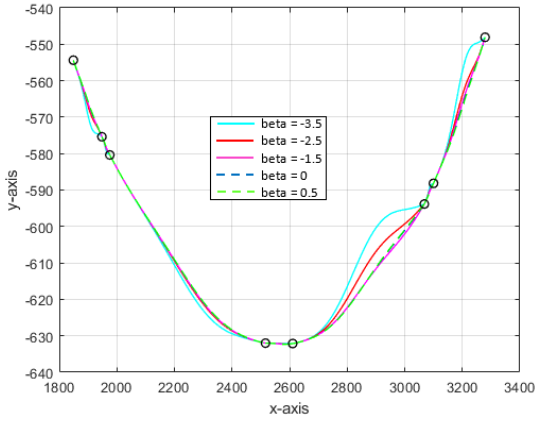

(b) Convexity-preserving interpolation with various β_i values.

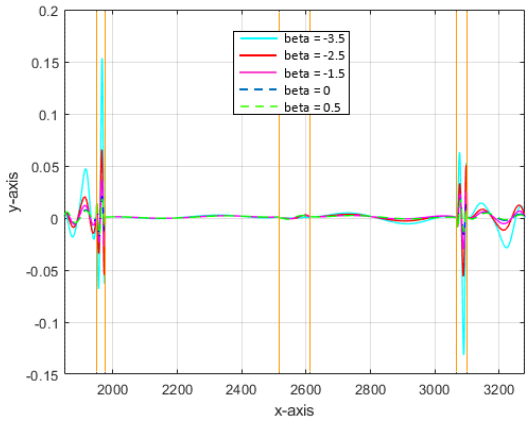

(c) Curvature plot for each curve in Figure 9b.

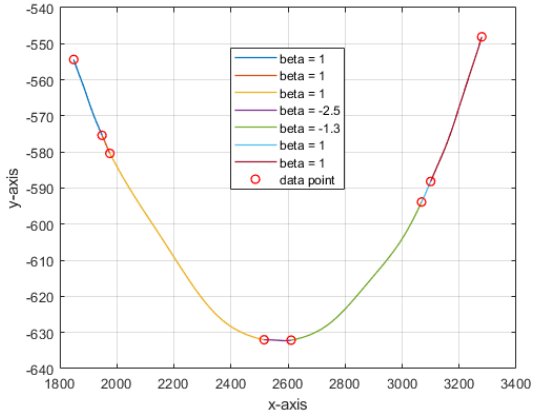

(d) Convex C^2 quintic trigonometric Bézier interpolating curve.

Figure 9. Interpolations for Example 5.6.

6. Conclusions

This study established new methods for preserving monotone or convex data. Quintic trigonometric Bézier curves with two shape parameters that control each end of the curve were used. Shape-preserving constraints were developed only on the left-end curves, whereas the right-end curve could be freely altered by users. This study also analyzed the curvature profiles to demonstrate visually pleasing interpolating curves, which improves the previous research by [30] that relied solely on visual comparison.

The proposed methods outperformed the existing schemes by reducing the wiggles and ensuring smooth increasing and decreasing trends, resulting in interpolation with less noticeable turning. Furthermore, the developed methods work well for both uniform and non-uniformly spaced data. The proposed methods also performed well with negative-valued data. Using a higher-degree Bézier curve, both the first- and second-order derivatives can be entirely calculated using the formula, thus reducing the complexity of the previous study. Furthermore, the higher-degree Bézier curve has a greater number

of control points, which increases curve control.

However, for constant data points, some values of β_i may cause the curvature plot to disconnect in the joint. Therefore, producing an interpolating curve that is not C^2 continuous. The basis functions used in this study can be extended to investigate the shape preservation of surfaces.

Use of AI tools declaration

The authors declare they have not used artificial intelligence (AI) tools in the creation of this article.

Acknowledgments

This research was supported by the Ministry of Higher Education Malaysia through the Fundamental Grant Scheme (FRGS/1/2023/STG06/USM/03/4) and the School of Mathematical Sciences, Universiti Sains Malaysia. The authors are very grateful to the anonymous referees for their valuable suggestions.

Conflict of interest

The authors declare that they have no competing interests in this paper.

References

1. M. Z. Hussain, M. Hussain, Visualization of data preserving monotonicity, *Appl. Math. Comput.*, **190** (2007), 1353–1364. http://dx.doi.org/10.1016/j.amc.2007.02.022
2. M. Sarfraz, M. Z. Hussain, M. Hussain, Shape-preserving curve interpolation, *Int. J. Comput. Math.*, **89** (2012), 35–53. http://dx.doi.org/10.1080/00207160.2011.627434
3. M. Hussain, A. Abd Majid, M. Z. Hussain, Convexity-preserving bernstein-bézier quartic scheme, *Egypt. Inform. J.*, **15** (2014), 89–95. http://dx.doi.org/10.1016/j.eij.2014.04.001
4. B. Kvasov, Monotone and convex interpolation by weighted quadratic splines, *Adv. Computat. Math.*, **40** (2014), 91–116. http://dx.doi.org/10.1007/s10444-013-9300-9
5. S. Karim, K. Pang, Monotonicity preserving using gc 1 rational quartic spline, *AIP Conf. Proc.*, **1482** (2012), 26–31. http://dx.doi.org/10.1063/1.4757432
6. A. Edeo, G. Gofeb, T. Tefera, Shape preserving C^2 rational cubic spline interpolation, *ASRJETS*, **12** (2015), 110–122.
7. S. Karim, Rational cubic spline interpolation for monotonic interpolating curve with C^2 continuity, *MATEC Web Conf.*, **131** (2017), 04016. http://dx.doi.org/10.1051/matecconf/201713104016
8. A. Ahmad, M. Misro, Preserving monotonicity of ball curve and it's curvature profile, *Proceedings of 6th IEEE International Conference on Recent Advances and Innovations in Engineering (ICRAIE)*, 2021, 1–6. http://dx.doi.org/10.1109/ICRAIE52900.2021.9704025
9. A. Tahat, A. Piah, Z. Yahya, Rational cubic ball curves for monotone data, *AIP Conf. Proc.*, **1750** (2016), 030021. http://dx.doi.org/10.1063/1.4954557

10. A. Ahmad, M. Misro, Curvature comparison of bézier curve, ball curve and trigonometric curve in preserving the positivity of real data, *AMCI*, **11** (2022), 12–20.
11. F. Pitolli, Ternary shape-preserving subdivision schemes, *Math. Comput. Simulat.*, **106** (2014), 185–194. http://dx.doi.org/10.1016/j.matcom.2013.04.003
12. P. Ashraf, M. Sabir, A. Ghaffar, K. Nisar, I. Khan, Shape-preservation of the four-point ternary interpolating non-stationary subdivision scheme, *Front. Phys.*, **7** (2020), 241. http://dx.doi.org/10.3389/fphy.2019.00241
13. A. Chand, N. Vijender, M. Navascués, Shape preservation of scientific data through rational fractal splines, *Calcolo*, **51** (2014), 329–362. http://dx.doi.org/10.1007/s10092-013-0088-2
14. P. Viswanathan, A. Chand, A fractal procedure for monotonicity preserving interpolation, *Appl. Math. Comput.*, **247** (2014), 190–204. http://dx.doi.org/10.1016/j.amc.2014.06.090
15. L. Peng, Y. Zhu, C^1 convexity-preserving piecewise variable degree rational interpolation spline, *J. Adv. Mech. Des. Syst.*, **14** (2020), JAMDSM0002. http://dx.doi.org/10.1299/jamdsm.2020jamdsm0002
16. M. Sarfraz, Visualization of positive and convex data by a rational cubic spline interpolation, *Inform. Sciences*, **146** (2002), 239–254. http://dx.doi.org/10.1016/S0020-0255(02)00209-8
17. M. Abbas, A. Abd Majid, J. Ali, Local convexity-preserving rational cubic spline for convex data, *Sci. World J.*, **2014** (2014), 391568. http://dx.doi.org/10.1155/2014/391568
18. Y. Zhu, C^2 rational quartic/cubic spline interpolant with shape constraints, *Results Math.*, **73** (2018), 127. http://dx.doi.org/10.1007/s00025-018-0883-9
19. M. Z. Hussain, M. Hussain, A. Waseem, Shape-preserving trigonometric functions, *Comp. Appl. Math.*, **33** (2014), 411–431. http://dx.doi.org/10.1007/s40314-013-0071-1
20. V. Bogdanov, Y. Volkov, Near-optimal tension parameters in convexity preserving interpolation by generalized cubic splines, *Numer. Algor.*, **86** (2021), 833–861. http://dx.doi.org/10.1007/s11075-020-00914-9
21. X. Han, Y. Ma, X. Huang, The cubic trigonometric bézier curve with two shape parameters, *Appl. Math. Lett.*, **22** (2009), 226–231. http://dx.doi.org/10.1016/j.aml.2008.03.015
22. S. Maqsood, M. Abbas, G. Hu, A. Ramli, K. Miura, A novel generalization of trigonometric bézier curve and surface with shape parameters and its applications, *Math. Probl. Eng.*, **2020** (2020), 4036434. http://dx.doi.org/10.1155/2020/4036434
23. M. Misro, A. Ramli, J. Ali, Quintic trigonometric bézier curve with two shape parameters, *Sains Malays.*, **46** (2017), 825–831. http://dx.doi.org/10.17576/jsm-2017-4605-17
24. M. Misro, A. Ramli, J. Ali, Quintic trigonometric bézier curve and its maximum speed estimation on highway designs, *AIP Conf. Proc.*, **1974** (2018), 020089. http://dx.doi.org/10.1063/1.5041620
25. V. Bulut, Path planning for autonomous ground vehicles based on quintic trigonometric bézier curve: path planning based on quintic trigonometric bézier curve, *J. Braz. Soc. Mech. Sci. Eng.*, **43** (2021), 104. http://dx.doi.org/10.1007/s40430-021-02826-8
26. J. Li, D. Zhao, An investigation on image compression using the trigonometric bézier curve with a shape parameter, *Math. Probl. Eng.*, **2013** (2013), 731648. http://dx.doi.org/10.1155/2013/731648

27. N. Ismail, M. Misro, Surface construction using continuous trigonometric bézier curve, *AIP Conf. Proc.*, **2266** (2020), 040012. http://dx.doi.org/10.1063/5.0018101

28. M. Z. Hussain, M. Hussain, Z. Yameen, A C^2-continuous rational quintic interpolation scheme for curve data with shape control, *J. Nati. Sci. Found. Sri*, **46** (2018), 341–354. http://dx.doi.org/10.4038/jnsfsr.v46i3.8486

29. S. Graiff Zurita, K. Kajiwara, K. Miura, Fairing of planar curves to log-aesthetic curves, *Japan J. Indust. Appl. Math.*, **40** (2023), 1203–1219. http://dx.doi.org/10.1007/s13160-023-00567-w

30. S. Mahzir, M. Misro, Shape preserving interpolation of positive and range-restricted data using quintic trigonometric bézier curves, *Alex. Eng. J.*, **80** (2023), 122–133. http://dx.doi.org/10.1016/j.aej.2023.08.009

AIMS Press